



RESEARCH ARTICLE

Novel de novo *POLR3B* mutations responsible for demyelinating Charcot–Marie–Tooth disease in Japan

Masahiro Ando¹ , Yujiro Higuchi¹, Jun-Hui Yuan¹ , Akiko Yoshimura¹, Ruriko Kitao², Takehiko Morimoto³, Takaki Taniguchi^{1,4}, Mika Takeuchi¹, Jun Takei¹, Yu Hiramatsu¹, Yusuke Sakiyama¹, Akihiro Hashiguchi¹, Yuji Okamoto^{1,5}, Jun Mitsui⁶, Hiroyuki Ishiura⁷, Shoji Tsuji^{6,8} & Hiroshi Takashima¹

¹Department of Neurology and Geriatrics, Kagoshima University Graduate School of Medical and Dental Sciences, Kagoshima, Japan

²Department of Neurology, National Hospital Organization Hakone Hospital, Kanagawa, Japan

³Department of Pediatrics, Asahigawaso Minamiehime Rehabilitation Hospital, Ehime, Japan

⁴Department of Neurology, Imakiire General Hospital, Kagoshima, Japan

⁵Department of Physical Therapy, School of Health Sciences, Faculty of Medicine, Kagoshima University, Kagoshima, Japan

⁶Department of Molecular Neurology, Graduate School of Medicine, The University of Tokyo, Chiba, Japan

⁷Department of Neurology, Faculty of Medicine, The University of Tokyo, Chiba, Japan

⁸Institute of Medical Genomics, International University of Health and Welfare, Chiba, Japan

Correspondence

Hiroshi Takashima, Department of Neurology and Geriatrics, Kagoshima University Graduate School of Medical and Dental Sciences, 8-35-1 Sakuragaoka, Kagoshima, Japan 890-8520. Tel: 81-99-275-5332; Fax: 81-99-265-7164; E-mail: thiroshi@m3.kufm.kagoshima-u.ac.jp

Funding Information

This work was supported by Grants-in-Aid from the Research Committee of Ataxia, Health Labour Sciences Research Grant, the Ministry of Health, Labour and Welfare, Japan (201610002B). This research is also supported by the Research program for conquering intractable disease from Japan Agency for Medical Research and Development (AMED) (201442014A, 201442071A, 17929553) and JSPS KAKENHI Grant Numbers JP18H02742, JP20K16604, JP21K15702, JP21H02842.

Received: 16 December 2021; Revised: 10 March 2022; Accepted: 24 March 2022

Annals of Clinical and Translational Neurology 2022; 9(5): 747–755

doi: 10.1002/acn3.51555

Introduction

Charcot–Marie–Tooth (CMT) disease is the most common type of inherited peripheral neuropathy characterized by clinical and genetic heterogeneity. The prevalence

Abstract

Background: Biallelic *POLR3B* mutations cause a rare hypomyelinating leukodystrophy. De novo *POLR3B* heterozygous mutations were recently associated with afferent ataxia, spasticity, variable intellectual disability, and epilepsy, and predominantly demyelinating sensorimotor peripheral neuropathy. **Methods:** We performed whole-exome sequencing (WES) of DNA samples from 804 Charcot–Marie–Tooth (CMT) cases that could not be genetically diagnosed by DNA-targeted resequencing microarray using next-generation sequencers. Using WES data, we analyzed the *POLR3B* mutations and confirmed their clinical features. **Results:** We identified de novo *POLR3B* heterozygous missense mutations in two patients. These patients presented with early-onset demyelinating sensorimotor neuropathy without ataxia, spasticity, or cognitive impairment. Patient 1 showed mild cerebellar atrophy and spinal cord atrophy on magnetic resonance imaging and eventually died of respiratory failure in her 50s. We classified these mutations as pathogenic based on segregation studies, comparison with control database, and in silico analysis. **Conclusion:** Our study is the third report on patients with demyelinating CMT harboring heterozygous *POLR3B* mutations and verifies the pathogenicity of *POLR3B* mutations in CMT. Although extremely rare in our large Japanese case series, *POLR3B* mutations should be added to the CMT-related gene panel for comprehensive genetic screening, particularly for patients with early-onset demyelinating CMT.

of CMT ranges from 9.7/100,000 to 82.3/100,000.¹ The disease is classified by motor nerve conduction velocity (MNCV) and mode of inheritance, as determined by family history. Generally, autosomal dominant CMT can be classified as demyelinating type (CMT1; median MNCV

<35 m/sec), axonal type (CMT2; median MNCV >45 m/sec), and dominant intermediate type (DI-CMT; median MNCV 35–45 m/sec).² To date, more than 100 genes have been associated with CMT and related disorders (<https://neuromuscular.wustl.edu/>). The common causative genes of CMT1 are *PMP22* (CMT1A, 1E), *MPZ* (CMT1B), *LITAF* (CMT1C), *EGR2* (CMT1D), *NEFL* (CMT1F), and *PMP2* (CMT1G) (<https://www.omim.org>). Other genes such as *FBRN5*, *C1orf94*, and *ITPR3* have also been found to cause CMT1.^{3–5}

Polymerase III (Pol III) transcribes small untranslated RNAs (such as tRNA, 5S RNA, 7SK RNA, and U6 RNA) and is involved in the regulation of important cellular processes, such as transcription, RNA processing, and translation. POLR3B is the second largest subunit of Pol III and, together with POLR3A, forms the catalytic center of the enzyme.⁶ In 2011, biallelic mutations in *POLR3B* were reported to cause a rare hypomyelinating leukodystrophy,⁷ whereas in 2021, de novo missense mutations in *POLR3B* were associated with afferent ataxia, spasticity, variable intellectual disability, and epilepsy, and predominantly demyelinating sensorimotor peripheral neuropathy.⁸ Heterozygous mutations in *POLR3B* could result in a demyelinating CMT phenotype without any additional neurological or extra-neurological involvement.⁹

In this study, we re-analyzed whole-exome sequencing (WES) data targeting *POLR3B* from more than 800 Japanese patients with CMT and described the clinical and genetic features of two patients harboring de novo heterozygous missense mutations in *POLR3B*.

Materials and Methods

Patients

We analyzed 2399 unrelated Japanese patients clinically diagnosed with CMT between 2007 and 2020. All patients with the demyelinating type were confirmed negative for *PMP22* duplication/deletion using fluorescence in situ hybridization or multiple ligation probe amplification. This study was approved by the institutional review board of Kagoshima University. All patients and family members provided informed consent for participation in the study.

Genomic DNA extraction

We extracted genomic DNA from peripheral blood or saliva using a Puregene Core Kit C (QIAGEN, Valencia, CA, USA) or Oragene DNA self-collection kit (DNA Genotek, Ottawa, Ontario, Canada) following the manufacturer's instructions.

Microarray chip sequencing and gene panel sequencing

From 2007 to 2012, mutation screening of 419 patients was carried out using a customized MyGeneChip® CustomSeq® Resequencing Array (Affymetrix, Inc., Santa Clara, CA, USA), targeting 30 CMT-related genes. Since 2012, Illumina Miseq (Illumina Inc., San Diego, CA, USA) and Ion Proton (ThermoFisher Scientific, Inc., Waltham, MA, USA), have been used to screen 60 and 72 known/candidate CMT-related genes, respectively. Until 2020, 438 CMT cases were analyzed using the Illumina Miseq system, whereas Ion Proton was used for 1542 cases. The detailed procedures have been described previously.^{10,11} *POLR3B* was not involved in any of these three in-house gene panels.

Whole-exome sequencing

Among the negative cases, 804 patients were further processed for WES via the Illumina Hiseq2000 platform (Illumina) or Ion Proton (ThermoFisher Scientific, Inc.). Sequencing data alignment (NCBI37/hg19) and variant calling were conducted with Burrows–Wheeler Aligner and SAM tools, or the Ion Reporter Server System. The called variants were annotated using the CLC Genomics Workbench software program (QIAGEN) and in-house R script. The details of our WES workflow have been described previously.¹²

Variant analysis and interpretation

We extracted all *POLR3B* (NM_018082.6) variants detected by WES from 804 CMT cases. These variants were checked against gnomAD (<https://gnomad.broadinstitute.org>), a Japanese control database (jMorp; <https://jmorp.megabank.tohoku.ac.jp/202109/>), and our in-house control database. Moreover, we performed six lines of computational analysis, consisting of SIFT/PROVEAN (<http://provean.jcvi.org/index.php>), PolyPhen-2 (<http://genetics.bwh.harvard.edu/pph2/>), Mutation Assessor (<http://mutationassessor.org/r3/>), FATHMM (<http://fathmm.biocompute.org.uk>), and Condel (<https://bbglab.irbbarcelona.org/fannsdbs/>), to predict the pathogenicity of the variants.

Protein stability and genetic tolerance analyses

Further protein stability analysis for these mutations were carried out using DynaMut (<http://biosig.unimelb.edu.au/dynamut/>), iMutant (<https://folding.biofold.org/i-mutant/i-mutant2.0.html>), and ConSurf (<https://consurf.tau.ac.il>).

Otherwise, MetaDome (<https://stuart.radboudumc.nl/metadome>) was used to measure the genetic tolerance of the entire *POLR3B* gene. All variants were validated using Sanger sequencing and interpreted according to the American College of Medical Genetics and Genomics (ACMG) standards and guidelines.¹³

Results

Clinical features

Patient 1

This was a female patient with non-consanguineous parents and no family history of peripheral neuropathy. Her father was diagnosed with amyotrophic lateral sclerosis (ALS) at the age of 80. Delayed motor milestone was noted in this patient when she was 1 year and 6 months old. At age 10 years, she was diagnosed with CMT and became wheelchair-bound at age 16. She also had scoliosis. When she was 34 years old, neurological findings showed predominant muscle weakness (manual muscle testing [MMT]: upper limb proximal 2/2, distal 0–1/0–1; and lower limb proximal 2/2, distal 0–1/0–1) and muscle atrophy in her extremities. She also showed distal dominant sensory impairment and absence of tendon reflexes. No intellectual disability, ataxia, spasticity, or seizure was noted. Her cognitive function at age 36 was normal (Hasegawa Dementia Scale–Revised, 29/30). Muscle biopsy at 10 years of age showed neurogenic changes (data not shown). Electrophysiological studies conducted at ages 36 and 46 revealed that none of the tested nerves were evoked except the musculocutaneous nerve. The MNCV of the musculocutaneous nerve was 26.5 m/sec, and the compound motor action potential was 1.84 mV. Her CMT type was not determined, but the reduced velocity of the musculocutaneous nerve suggested the possibility of demyelinating CMT. Needle electromyography revealed fibrillation potentials/positive sharp waves in her flexor digitorum profundus muscle. High-amplitude and long-duration motor unit action potentials were evident in her biceps brachii. Her electrophysiological data are shown in Table 1. Whole-body computed tomography at age 51 showed marked muscle atrophy of the upper and lower extremities. Brain magnetic resonance imaging (MRI) at ages 47 and 53 showed nonprogressive mild cerebellar atrophy and left cerebellopontine angle meningioma. No evidence of cerebral atrophy was observed. Her cervical spine MRI at age 50 revealed spinal cord atrophy (Fig. 1).

The patient also developed respiratory dysfunction. Her vital capacity was 2.04 L (72%) at age 28 and 0.88 L (34%) at age 46. This patient refused mechanical respiratory support and died of acute progression of chronic respiratory failure at the age of 54.

Table 1. Electrophysiological findings of two patients with *POLR3B* heterozygous variants.

Patient	Family 1		Family 2	
	II-2		II-2	
Exam age (y.o)	36	46	8	10
Median nerve				
MNCV (m/sec)	NE	NE	22.2	21
CMAP (mV)	NE	NE	2.2	3
SCV (m/sec)	NE	NE	NE	NE
SNAP (μ V)	NE	NE	NE	NE
Ulnar nerve				
MNCV (m/sec)	n.a	NE	25.3	22.8
CMAP (mV)	n.a	NE	0.9	1.8
SCV (m/sec)	n.a	NE	NE	NE
SNAP (μ V)	n.a	NE	NE	NE
Tibial nerve				
MNCV (m/sec)	NE	NE	n.a	NE
CMAP (mV)	NE	NE	n.a	NE
Peroneal nerve				
MNCV (m/sec)	n.a	n.a	NE	NE
CMAP (mV)	n.a	n.a	NE	NE
Sural nerve				
SCV (m/sec)	NE	NE	NE	NE
SNAP (μ V)	NE	NE	NE	NE
Musculocutaneous nerve				
MNCV (m/sec)	n.a	26.5	n.a	n.a
CMAP (mV)	n.a	1.8	n.a	n.a
nEMG				
Fibs/PSW	+	–	n.a	–
MUP Amp	High	High	High	High
MUP Dur	Long	Long	Long	Long

Normal range: median CMAP >3.1 mV; median MCV >49.6 m/sec; median SNAP >7.0 μ V; median SCV >47.2 m/sec; tibial CMAP >4.4 mV; tibial MCV >41.7 m/sec; sural SNAP >5.0 μ V; sural SCV >40.8 m/sec; musculocutaneous CMAP and MCV have not been determined. MNCV, motor nerve conduction velocity; CMAP, compound motor action potential; SCV, sensory nerve conduction velocity; SNAP, sensory nerve action potential; NE, not evoked; n.a, not available; Fibs, fibrillation potentials; PSWs, positive sharp waves; nEMG, needle electromyography; MUP Amp, motor unit potential amplitude; MUP Dur, motor unit potential duration.

Patient 2

The patient was a 26-year-old female. Her parents were not consanguineous, and no similar symptoms were found in her family members. Her initial symptom was delayed motor milestone. At 18 months of age, she began walking independently but developed walking difficulties half a year later. She was diagnosed with CMT at the age of 8 due to marked muscle weakness and atrophy in the distal extremities, foot deformity, and loss of tendon reflexes. Her median MNCV decreased (22 m/sec) on nerve conduction study and was thus diagnosed with demyelinating CMT. Sural nerve pathology at 8 years of

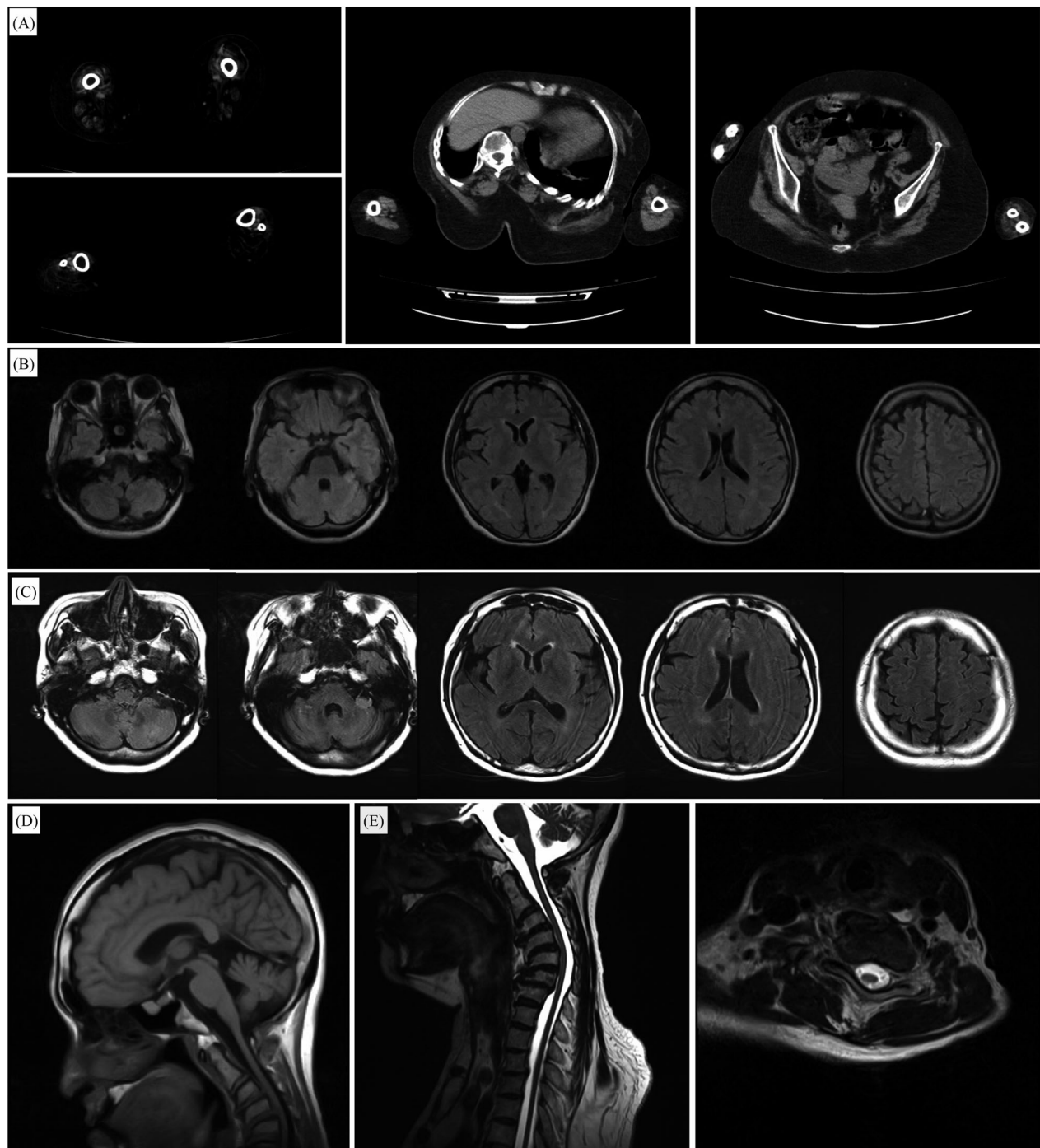


Figure 1. Radiological findings in patient 1 with *POLR3B* Arg469Cys. (A) Her computed tomography (CT) at age 51 shows marked muscle atrophy in both distal and proximal lower limbs, and in upper limbs with distal predominance. (B) Brain MRI axial slice at age 47, suggesting mild cerebellar atrophy and left cerebellopontine angle meningioma. (C) Brain MRI axial slice at age 53, with no notable changes in her cerebellar volume and meningioma. (D) Brain MRI sagittal slice at age 47, showing atrophy of cerebellar but not in corpus callosum. (E) Cervical spine MRI at age 50 showing cervical spinal cord atrophy.

age showed a complete absence of large myelinated fibers, but small myelinated fibers and normal unmyelinated fibers were observed.¹⁴ Her neurological,

electrophysiological, and pathological findings at age 8 were reported by Fukuda et al.¹⁴ Nerve conduction test at age 10 showed lower median (21 m/sec) and ulnar

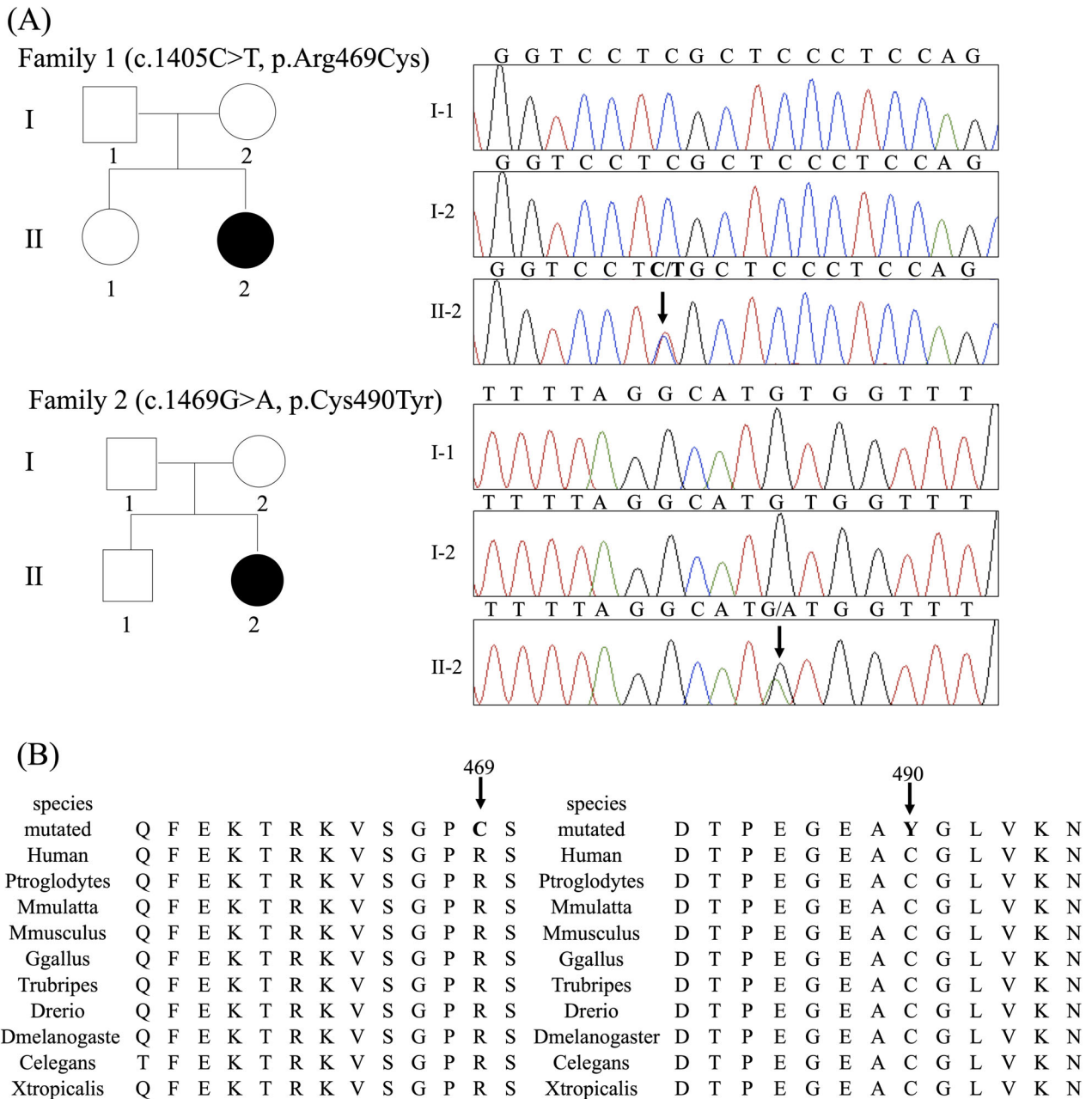


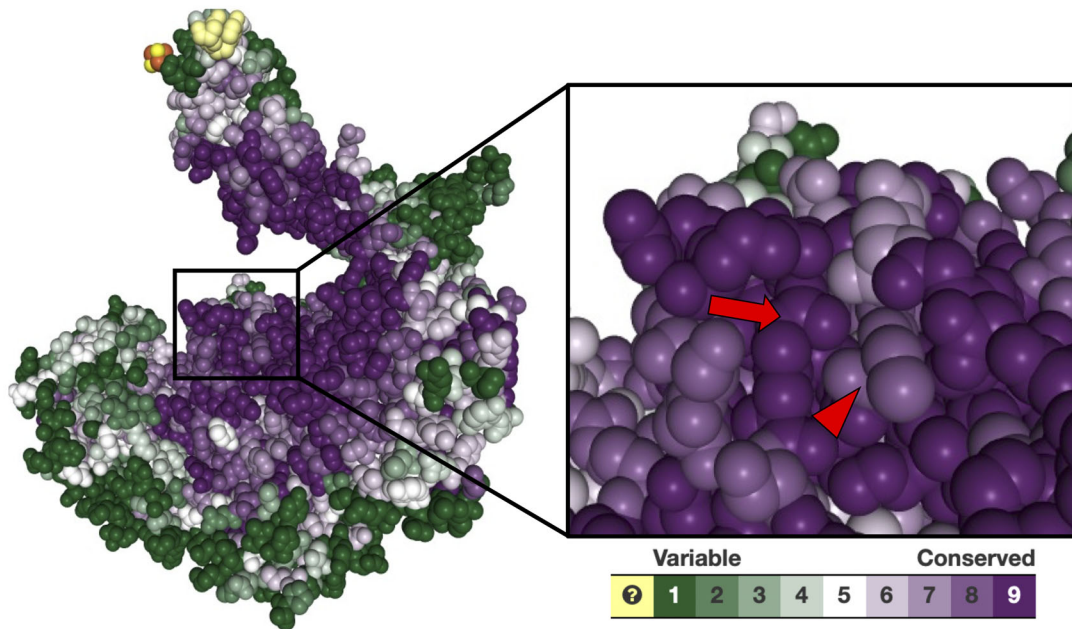
Figure 2. Two pedigrees with de novo *POLR3B* heterozygous variants. (A) Family tree and segregation study of sporadic CMT with de novo *POLR3B* heterozygous variants. (B) Mutated residues of *POLR3B* are highly conserved across multiple species.

(22.8 m/sec) MNCV than those at age 8 (Table 1). She exhibited significant muscle weakness in the tibialis anterior muscle, which required a brace, but she was able to walk independently at age 26. Her MMT was 3–4 in the fingers and 4–5 in the proximal muscles. No intellectual disability, ataxia, spasticity, or seizure was noted in this patient.

Genetic findings

From the two patients with demyelinating CMT, we identified two novel *POLR3B* heterozygous variants, c.1405C>T (p.Arg469Cys, NM_018082.6; chr12: 106824192C>T, GRCh37/hg19) and c.1469G>A (p.Cys490Tyr; chr12: 106826100G>A) from our WES data.

(A)



(B)

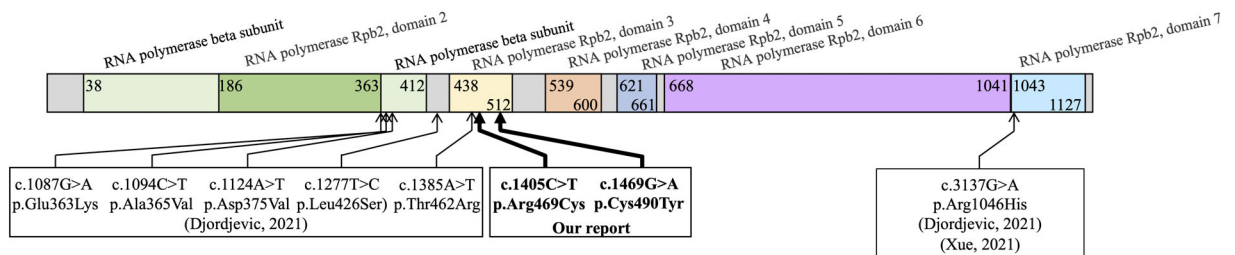
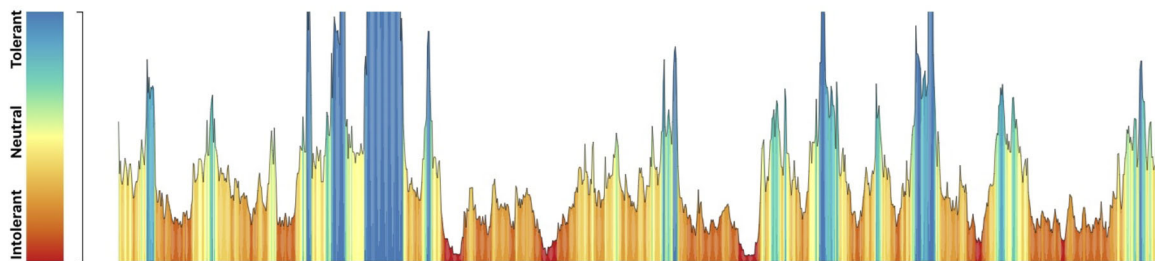


Figure 3. Location of *POLR3B* Arg469 / Cys490, and mutation tolerance landscape. (A) Location of Arg469 (arrow head) and Cys490 (arrow). Mutations both locate at a highly conserved region, with conservation scores at 9 (Arg469) and 8 (Cys490), respectively in the ConSurf analysis. These residues locate very close together on protein surface. (B) Mutation tolerance landscape and domains of *POLR3B*. Both mutations locate in the RNA polymerase Rpb2, domain 3, which is highly intolerance to genomic variants. The previously reported mutations are also labeled.

We present the pedigrees of these patients in Figure 2A. Segregation studies were carried out on both pedigrees, and these variants were not detected in their parents. The parentage of each pedigree was verified based on rare variants identified using whole-exome sequencing. These variants were thus considered as *de novo* (ACMG criteria; PS2). Meanwhile, we could not identify

suspected variants from any other known disease-causing genes. Both variants were absent in the public databases (ACMG criteria; PM2) and our in-house control database (ACMG criteria; PS4-moderate). The Arg469 and Cys490 residues are highly conserved throughout multiple species (Fig. 2B). Computational analyses (SIFT, PROVEAN, PolyPhen-2, Mutation Assessor, FATHMM, and Condel)

using multiple tools (ACMG criteria; PP3) indicate these variants to have damaging effects.

ConSurf predicted high conservation scores for Arg469 and Cys490 of between 8 and 9 and found them located in close proximity to each other on the protein surface (Fig. 3A). The DynaMut prediction outcome of Arg469Cys ($\Delta\Delta G$: -1.554 kcal/mol) showed a destabilizing effect. However, Cys490Tyr ($\Delta\Delta G$: 0.866 kcal/mol) exhibited a stabilizing effect. MetaDome demonstrated that both variants were located on the RNA polymerase Rpb2, domain 3, which is highly intolerant to genomic variants (Fig. 3B). Furthermore, cases with these variants exhibited a CMT1 phenotype, which was consistent with this genetic etiology (ACMG criteria; PP4). Altogether, we classified these variants as pathogenic according to the ACMG guideline. These genetic findings are shown in Table 2. All *POLR3B* variants in this study identified are shown in Tables S1 and S2.

Discussion

Based on WES data from more than 800 Japanese CMT cases, we identified two novel de novo missense mutations in *POLR3B*, c.1405C>T (p.Arg469Cys) and c.1469G>A (p.Cys490Tyr), from two nonconsecutive patients with demyelinating CMT.

POLR3B is the second largest subunit of Pol III. The biallelic mutation in *POLR3A*, which encodes the largest

Pol III subunit, is known to cause tremor-ataxia with central hypomyelination, hypodontia, hypogonadotropic hypogonadism (4H syndrome), and leukodystrophy with oligodontia.¹⁵ In 2011, biallelic mutations in *POLR3B* were reported to cause a rare hypomyelinating leukodystrophy.⁷ Such types of leukodystrophy are now referred to as *POLR3*-related leukodystrophy, including leukodystrophy caused by biallelic mutations in *POLRIC* or *POLR3K*.^{16,17} The typical neurological features of patients with *POLR3B*-associated leukodystrophy mainly implicate the central nervous system, whereas no obvious peripheral neuropathy has been reported. In 2021, Djordjevic et al. reported that multiple de novo heterozygous variants of *POLR3B*, namely, c.1087G>A [p.Glu363Lys], c.1094C>T [p.Ala365Val], c.1124A>T [p.Asp375Val], c.1277T>C [p.Leu426Ser], c.1385C>G [p.Thr462Arg], and c.3137G>A [p.Arg1046His], were linked to a broad spectrum of clinical phenotypes, including demyelinating neuropathy, ataxia, spasticity, and variable intellectual disability and epilepsy. They further evaluated the assembly of specific RNA Pol III subunits in human embryonic kidney cell line 293 cells using affinity purification and mass spectrometry to define the impact of the de novo variant. They stated that the heterozygous mutations in *POLR3B* may cause disruption in the association of one or two enzyme subunits, possibly with a dominant-negative effect, and exert pathogenicity.

Table 2. Genetic findings of *POLR3B* Arg469Cys and Cys490Tyr.

<i>POLR3B</i> variant (NM_018082.6)	c.1405C>T		c.1469G>A	
Amino acid change	p.Arg469Cys		p.Cys490Tyr	
Zygoty	Heterozygous		Heterozygous	
Allele frequency-gnomAD	0		0	
Allele frequency-jMorp	0		0	
Our control	–		–	
SIFT/prediction	0	Damaging	0	Damaging
PROVEAN/prediction	–7	Deleterious	–10.37	Deleterious
Polyphen2/prediction	1	Damaging	1	Damaging
MutationAssesor/prediction	4.265	Damaging	3.95	Damaging
FATHMM/prediction	–4.43	Benign	–1.5	Benign
Condel/prediction	0.745	Damaging	0.777	Damaging
Consurf/prediction	9	Hightly conserved	8	Hightly conserved
Dynamut				
$\Delta\Delta G$ /prediction	–1.554 kcal/mol	Destabilizing	0.866 kcal/mol	Stabilizing
$\Delta\Delta G$ (ENCOM)/prediction	–0.678 kcal/mol	Destabilizing	0.347 kcal/mol	Destabilizing
iMutant				
RI/stability	5	Decrease	3	Increase
ACMG				
Population data	PS4(M), PM2		PS4(M), PM2	
In silico data	PP3		PP3	
De novo data	PS2		PS2	
Other data	PP4		PP4	
Criteria	Pathogenic		Pathogenic	

Xue et al.⁹ found a case of demyelinating CMT with a *POLR3B* heterozygous mutation (c.3137G>A [p.Arg1046His]) had no additional neurological or extra-neurological involvement. This phenotypic similarity strongly reinforced the possibility that *POLR3B* missense heterozygous mutations could cause demyelinating CMT. In the present study, the two cases with novel and pathogenic *POLR3B* variants also shared a comparable phenotype of early-onset demyelinating CMT, as in previous reports. A segregation study of both pedigrees suggested that these variants were de novo, which is also consistent with the original report.

Although no evidence of cerebellar ataxia, spasticity, seizures, or dementia was identified in either of our patients, the MRI study of patient 1 showed mild atrophy in the cerebellum and spinal cord. This radiological finding is consistent with the broad spectrum of clinical phenotypes described by Djordjevic et al. Although the father of patient 1 was clinically suspected with ALS at an old age, their clinical phenotypes were completely different, and no suspicious variant was identified in any ALS-related genes using the WES data of patient 1 and her father. More likely, her father developed sporadic ALS incidentally.

Since we were unable to perform functional studies on these mutations due to technical and material limitations, we evaluated the pathogenicity using several in silico analyses and protein stability testing. The results showed that these mutations were located within a highly intolerant domain of *POLR3B* and closely located on the conserved region of the protein surface, suggesting potential damaging effects. Based on all these findings, we believe that the two de novo mutations are causative for patients with demyelinating CMT.

This article is the third report on patients with demyelinating CMT associated with *POLR3B* heterozygous mutations. Our findings further verify the pathogenicity of the de novo heterozygous mutations in *POLR3B* and highlight the role of this gene in the genetic spectrum of CMT1. These findings also broaden the clinical spectrum of *POLR3B*-related phenotypes. Although extremely rare in our large Japanese cohort, the CMT-related gene panel for comprehensive genetic screening should be performed, particularly for patients with early-onset demyelinating CMT.

Acknowledgment

The authors appreciate Tomoko Ohnishi at Kagoshima University, for their great technical assistance. The authors are supported by Enago (www.enago.jp) for reviewing the English in this report. We appreciate the Division of Gene Research, Research Support Centre, Kagoshima University, for the use of their facilities. This

work was supported by Grants-in-Aid from the Research Committee of Ataxia, Health Labour Sciences Research Grant, the Ministry of Health, Labour and Welfare, Japan (201610002B). This research is also supported by the Research program for conquering intractable disease from Japan Agency for Medical Research and Development (AMED) (201442014A, 201442071A, 17929553) and JSPS KAKENHI Grant Numbers JP18H02742, JP20K16604, JP21K15702, JP21H02842.

Conflict of Interest

All authors declare that there is no conflict of interest.

References

1. Braathen GJ, Sand JC, Lobato A, Høyer H, Russell MB. Genetic epidemiology of Charcot-Marie-Tooth in the general population. *Eur J Neurol*. 2011;18:39-48.
2. Stojkovic T. Hereditary neuropathies: an update. *Rev Neurol (Paris)*. 2016;172(12):775-778.
3. Auer-Grumbach M, Weger M, Fink-Puches R, et al. Fibulin-5 mutations link inherited neuropathies, age-related macular degeneration and hyperelastic skin. *Brain*. 2011;134(Pt 6):1839-1852.
4. Sun SC, Ma D, Li MY, et al. Mutations in *C1orf194*, encoding a calcium regulator, cause dominant Charcot-Marie-Tooth disease. *Brain*. 2019;142(8):2215-2229.
5. Rönkkö J, Molchanova S, Revah-Politi A, et al. Dominant mutations in *ITPR3* cause Charcot-Marie-Tooth disease. *Ann Clin Transl Neurol*. 2020;7(10):1962-1972.
6. Dumay-Odelot H, Durrieu-Gaillard S, Da Silva D, et al. Cell growth- and differentiation-dependent regulation of RNA polymerase III transcription. *Cell Cycle*. 2010;18:3687-3699.
7. Tétreault M, Choquet K, Orcesi S, et al. Recessive mutations in *POLR3B*, encoding the second largest subunit of pol III, cause a rare hypomyelinating leukodystrophy. *Am J Hum Genet*. 2011;89(5):652-655.
8. Djordjevic D, Pinard M, Gauthier MS, et al. De novo variants in *POLR3B* cause ataxia, spasticity, and demyelinating neuropathy. *Am J Hum Genet*. 2021;108(1):186-193.
9. Xue YY, Cheng HL, Dong HL, et al. A de novo variant of *POLR3B* causes demyelinating Charcot-Marie-Tooth disease in a Chinese patient: a case report. *BMC Neurol*. 2021;21(1):402.
10. Hashiguchi A, Higuchi Y, Nomura M, et al. Neurofilament light mutation causes hereditary motor and sensory neuropathy with pyramidal signs. *J Peripher Nerv Syst*. 2014;19:311-316.
11. Yoshimura A, Yuan JH, Hashiguchi A, et al. Genetic profile and onset features of 1005 patients with Charcot-

- Marie-Tooth disease in Japan. *J Neurol Neurosurg Psychiatry*. 2019;90(2):195-202.
12. Ando M, Okamoto Y, Yoshimura A, et al. Clinical and mutational spectrum of Charcot-Marie-Tooth disease type 2Z caused by *MORC2* variants in Japan. *Eur J Neurol*. 2017;24(10):1274-1282.
 13. Richards S, Aziz N, Bale S, et al. Standards and guidelines for the interpretation of sequence variants: a joint consensus recommendation of the American College of Medical Genetics and Genomics and the Association for Molecular Pathology. *Genet Med*. 2015;17(5):405-424.
 14. Fukuda M, Morimoto T, Suzuki Y, Kida K, Ohnishi A. Congenital neuropathy with the absence of large myelinated fibers. *Pediatr Neurol*. 2000;23(4):349-351.
 15. Bernard G, Chouery E, Putorti ML, et al. Mutations of *POLR3A* encoding a catalytic subunit of RNA polymerase pol III cause a recessive hypomyelinating leukodystrophy. *Am J Hum Genet*. 2011;89(3):415-423.
 16. Thiffault I, Wolf NI, Forget D, et al. Recessive mutations in *POLR1C* cause a leukodystrophy by impairing biogenesis of RNA polymerase III. *Nat Commun*. 2015;6:7623.
 17. Dorboz I, Dumay-Odelot H, Boussaid K, et al. Mutation in *POLR3K* causes hypomyelinating leukodystrophy and abnormal ribosomal RNA regulation. *Neurol Genet*. 2018;4(6):e289.

Supporting Information

Additional supporting information may be found online in the Supporting Information section at the end of the article.

Table S1. Genomic variants of *POLR3B* detected by WES.
Table S2. Variant interpretation with ACMG guideline for *POLR3B* variants detected by WES.